Proceeding of the IEEE
International Conference on Robotics and Biomimetics
Dali, China, December 2019

Study on Self-Takeoff of a Flapping Robot without Running: Influence of the Initial Pitch Angle on the Takeoff Trajectory

Terukazu Sato, Takahiro Nakano, and Naoyuki Takesue
Tokyo Metropolitan University
sato-terukazu@ed.tmu.ac.jp, nakano-takahiro@ed.tmu.ac.jp, ntakesue@tmu.ac.jp

***Abstract*— Recently, research on flapping robots inspired by the behavior of insects and birds has become a focus of attention in the fields of robotics and biomimetics. However, most flapping robots require an operator or an assistance device to take off. The goal of this study was to develop a flapping robot that can achieve self-takeoff without running and can be used like a drone. This paper describes the development and evaluation of the flapping robot developed with this aim. The developed robot can generate a thrust that exceeds its own weight with a simple flapping mechanism and a lightweight design. The airspeed was simulated using the thrust measured with a force sensor and the resistance coefficient estimated in a gliding experiment, and it was found to exceed the minimum airspeed required to achieve takeoff 0.3 s from the onset of flapping. The result of the takeoff experiment demonstrated that takeoff was possible if the initial pitch angle was high. However, the pitch angle decreased immediately after takeoff due to the pitching moment generated by the flapping motion. The moment on the tail wing was not enough for the robot to maintain a horizontal posture at low airspeeds during takeoff. It was concluded that the robot requires a control mechanism for the pitching moment generated by the flapping motion and/or accelerators that function without flapping during takeoff, such as hind limbs. Therefore, the parameters required for the design of actuated hind limbs were estimated.**

***Index Terms*— Flapping robot, Self-takeoff, Micro aerial vehicle**

I. Introduction

Recently, research on flapping robots that mimic insects and birds has attracted attention in the fields of robotics and biomimetics. Such robots are called micro aerial vehicles (MAVs), and many teams have been developing robots of this type [1]. The wings of birds generate lift and thrust forces, and it is possible for them to glide without flapping at a sufficiently high airspeed. MAVs show excellent motion performance, including their acceleration and turning ability, and they require little to no takeoff and landing distance.

Furthermore, unmanned aerial vehicles called drones, which have advanced functions such as automatic navigation, are used in various fields such as environmental investigation, disaster relief, and bridge inspection. As a result of improvement of various technologies, such as battery, motor, and control technologies, it has become possible to fly drones loaded with cameras and sensors for a long time. However, there remain problems such as payload, cruising distance, noise, and safety in the case of a crash. Flapping robots are expected to solve such problems. These robots can save flying energy when gliding, and unpleasant noise can be reduced because there is no need to rotate propellers at a high speed. Additionally, their safety level when the robot crashes is better than that of traditional drones.

Flapping robots offer many advantages and are expected to open the door to new fields of application rather than simply replacing drones. For example, they would enable natural environment investigation because of their ability to mimic birds in shape and motion. For the same reason, they could also be used to safely ward off birds by posing as a predatory bird; this application would be especially useful at airports where birds are a safety hazard.

For a flapping robot to be used like a drone, it must be able to take off by remote control, fly at a certain speed, reach a target point, and land. However, most flapping robots cannot achieve takeoff by remote control but must be launched by an operator or an assistance device. The goal of this study was to develop a flapping robot that can achieve self-takeoff without running; this means that the robot must take off without using a catapult, being thrown by hand, or rolling with wheels.

Examples of flapping robots that can achieve self-takeoff without running include the Nano hummingbird [2], DelFly [3](Fig. I), and WiFly [4]. They flap their wings in a posture with their flapping axis aligned vertically and take off with a lift force equal to the generated thrust minus their own weight. They were designed to be stable in such a posture; however, they cannot directly transition from this posture to horizontal flight. The WiFly solves this problem by using a mechanism to move the center of gravity to switch to horizontal flight. However, one drawback of existing flapping robots is that they consume a lot of energy to reach a sufficient altitude and airspeed, as with general vertical takeoff and landing aircraft (VTOL). During takeoff, birds accelerate mainly by use of their hind limbs [5], which generate an initial velocity in both the horizontal and vertical directions, and gain lift from their airspeed, thereby initiating flight by expending less energy than their robotic counterparts.

In this study, a flapping robot that generates a thrust exceeding its own weight was developed. Its static thrust was then measured, and its performance was evaluated through gliding and takeoff experiments.

978-1-7281-6321-5/19//$31.00 ©2019 IEEE

(1) Nano hummingbird [2]

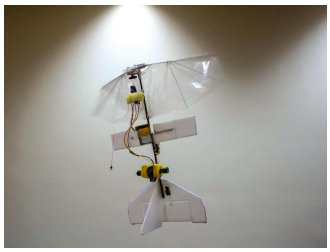

(2) DelFly Explorer [3]

Fig. 1. Self-takeoff flapping robots

II. Mechanical Design

The flapping robot was developed based on a bottom-up design, because parts must be carefully chosen to achieve an overall lightweight device. A brushless direct current (BLDC) motor for small lightweight drones that have a high power ratio was selected to drive the flapping mechanism. A gear reducer and a flapping mechanism were designed in accordance with this motor. The flapping mechanism is a simple lever crank mechanism, as shown in Fig. 2.

The frame of the gear reducer unit was made of carbon-fiber-reinforced plastic (CFRP), and the wing structures were made of carbon rods. Strong lightweight nylon fabric called Ripstop was used as the wing film. The wing film was stretched only over the upper surface of the ribs. The flapping mechanism was fabricated from nylon plastic containing short carbon fibers printed with a three-dimensional (3D) printer to ensure it was lightweight. For flying stability, the design of the flapping wings was based on the design elements of the wings of general aircraft that use dihedral angles and swept wings. A single triangular tail wing was added in imitation of a bird. It is controlled by two linear actuators for the pitch and yaw axes. A photograph and computer-aided design (CAD) model of the developed flapping robot are respectively shown in Fig. 3 and Fig. 4. The specifications of the robot are given in Table I.

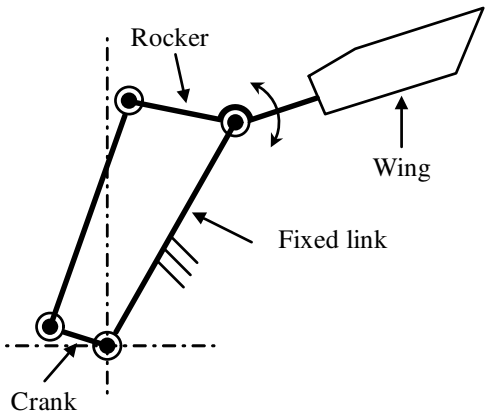

Fig. 2. Flapping mechanism

Fig. 3. Photograph of the developed flapping robot

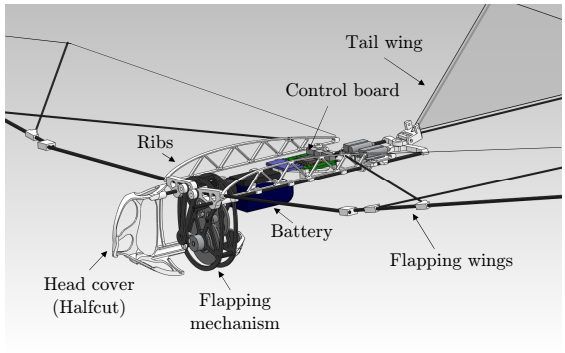

Fig. 4. CAD model of the flapping robot

TABLE I
Specifications of the Flapping Robot

Wingspan	760 mm
Total weight	85 g
Gear ratio	144:1 reduction
BLDC motor spec.	7000 KV, 36 W, 6 g
Li-poly battery spec.	11.1 V, 180 mAh, 19 g

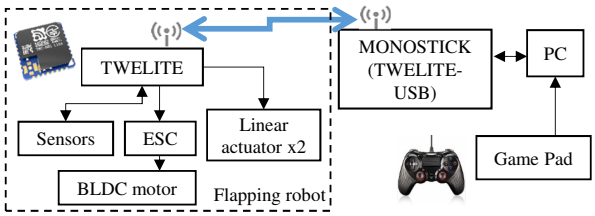

Fig. 5. System diagram

III. Electrical Design

The TWELITE, which is a wireless module with a built-in microcontroller, was used as a control system for the flapping robot. The control system can remotely control the robot from a distance of approximately 1 km using a personal computer (PC) and feedback from an orientation sensor and a flapping angle sensor mounted on the flapping robot. The system configuration is shown in Fig. 5.

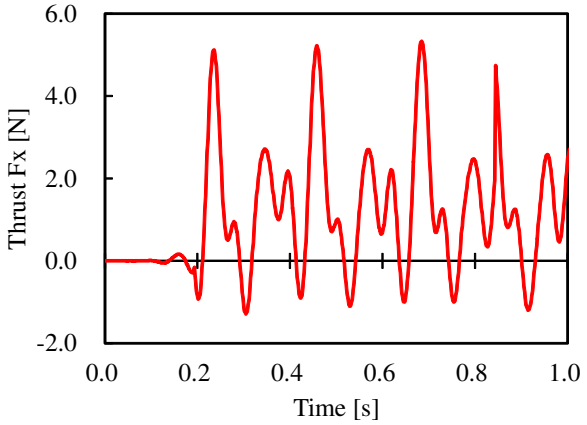

Fig. 6. Thrust force F_x

IV. Experiment and Discussion

A. Static thrust measurement

To measure the static thrust generated by the flapping robot, it was mounted on a force sensor. The flapping robot was made to begin flapping, and the force was measured in the no-airspeed condition, which is similar to the conditions of self-takeoff. In the coordinate system of the flapping robot, the forward force is defined as the thrust F_x, and the upward force defined as the lift F_z. The measured thrust over time is shown in Fig. 6, and the thrust and lift averaged over 1 s are given in Table II. The results revealed that the generated thrust was greater than the weight of the robot (0.83 N). It was thus confirmed that the robot can fly against its own weight when it is in a vertical posture. Very little lift was generated because the flapping motions in the up and down strokes were almost symmetric.

B. Gliding experiment

A motion capture system was used to measure the airspeed of the flapping robot during gliding. A marker for the motion capture was attached to the head of the flapping robot, and the velocity was calculated from the trajectory of the acquired position data. The airspeed and lowering speed are given in Table III.

The relationship between the wing loading and the airspeed can be expressed as follows [6]:

$$\frac{W}{S} = 0.38V^2, \tag{1}$$

TABLE II
Summary of Static Thrust Experiment

Flapping frequency(Hz)	4.5
F_x(N)	1.26
F_z(N)	−0.04

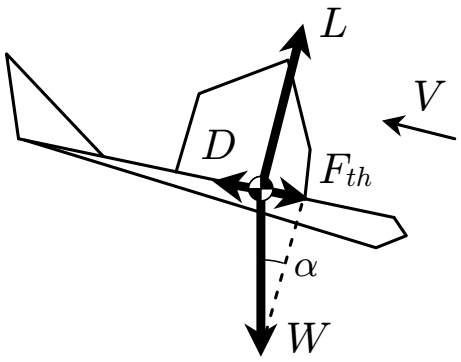

Fig. 7. Forces on gliding airplane

where W is the weight [N], S is the wing area [m^2], and V is the airspeed [m/s]. From this equation, the airspeed of the flapping robot was $V = 5.56$ m/s, which is almost equal to the measured gliding airspeed of 5.45 m/s. This airspeed is the minimum airspeed to achieve takeoff.

During gliding, the drag D is balanced with the component $F_{\rm th}$ of the weight W in the direction parallel to the roll axis of the flapping robot at a steady state (Fig. 7). Therefore, the drag D and $F_{\rm th}$ can be determined from the following equations:

$$D = \frac{1}{2}C_D S\rho V^2 \tag{2}$$

$$F_{\rm th} = W\sin\alpha, \tag{3}$$

where C_D is the drag coefficient, ρ is the density of air [kg/m^3], α is the angle of the roll axis of the robot with respect to the vertical. From the experiment results given in Table III, the angle and drag coefficient were obtained as $\alpha = \sin^{-1}(V_z/V) = 0.28$ rad and a drag coefficient of $C_D{}' = \frac{1}{2}C_D S\rho = 6.85\times10^{-3}$.

The velocity of the flapping robot starting from rest was simulated using the drag coefficient $C_D{}'$ and the thrust F_x. The motion of the flapping robot was assumed to be one-dimensional in the propulsion direction, and the velocity obtained by numerically solving the following equation of motion is shown in Fig. 8:

$$ma = F_x - D, \tag{4}$$

where a is the acceleration of the robot.

The velocity exceeded 5.5 m/s approximately 0.3 s after flapping began and eventually converged to approximately 12.3 m/s. However, the velocity of an actual robot designed in this manner would be slower because as the airspeed

TABLE III
Gliding Velocity

Airspeed V(m/s)	5.45
Lowering speed V_z(m/s)	1.50

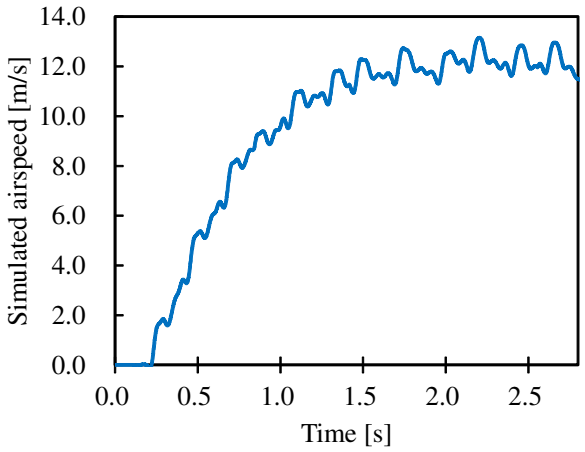

Fig. 8. Velocity simulation

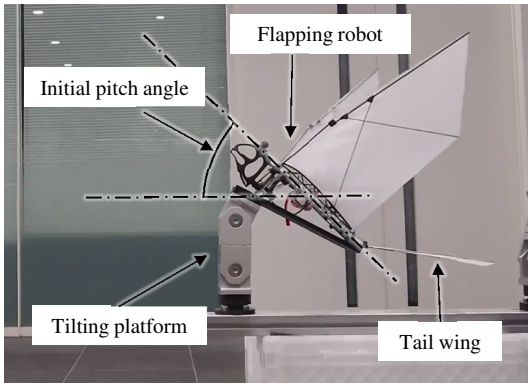

Fig. 9. Takeoff experiment to determine the effect of the initial pitch angle on the robot motion

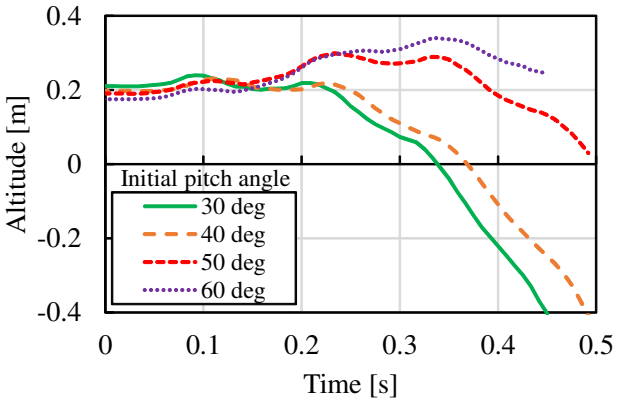

Fig. 10. Altitude after takeoff

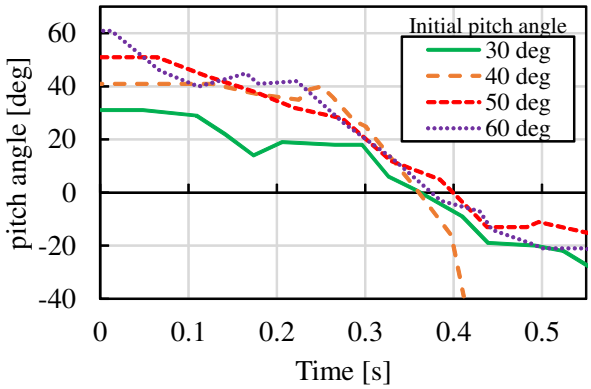

Fig. 11. Pitch angle after takeoff

increases, the angle of attack of the flapping wing and the thrust decrease.

C. Takeoff experiment

The flapping robot was placed on a platform with a given initial pitch angle, and experiments were conducted to examine how its ability to take off without running was affected by the initial pitch angle (Fig. 9). The trajectory during takeoff was measured with the motion capture system. The altitude of the flapping robot with respect to the origin of the camera coordinate system is plotted over time for different initial pitch angles in Fig. 10. The different initial pitch angles showed different behavior from approximately 0.15 s after the beginning of flapping. The altitude of the flapping robot increased by approximately 150 mm from the initial altitude when the initial pitch angle was 60°. These results indicate that takeoff without running is possible if the initial pitch angle is sufficiently high. The pitch angle of the flapping robot after takeoff measured by the orientation sensor mounted on the robot is shown in Fig. 11. The results demonstrate that the robot took on a horizontal posture approximately 0.37 s after the onset of flapping regardless of the initial pitch angle and the pitch angle continued to decrease after that.

The time evolution of the airspeed for each initial pitch angle is shown in Fig. 12. In the case of an initial pitch angle of 30°, the robot accelerated to 4.6 m/s after 0.3 s. However, the airspeed was less than the velocity obtained in the simulation, which was 5.5 m/s at 0.3 s. At higher initial pitch angles, the flapping robot accelerated more slowly because it had to counter gravity. However, at smaller initial pitch angles, the flapping robot could not rise after takeoff, and the altitude decreased rapidly. Therefore, the initial pitch angle can be regarded as a parameter that determines how the mechanical energy produced by the flapping is divided into kinetic and potential energy.

D. Moment about the center of gravity

Fig. 11 demonstrates that even if the initial pitch angle is high, the pitch angle of the robot decreases immediately after takeoff. It was considered that the pitching moment is generated by the flapping of the wings of the robot. The pitching moment M_{flg} about the center of gravity of the

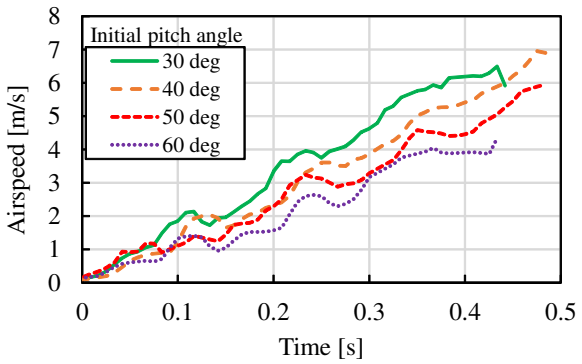

Fig. 12. Velocity after takeoff

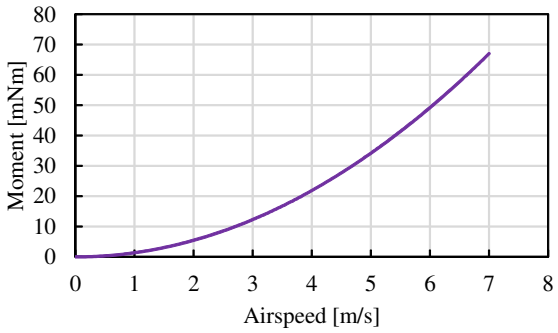

Fig. 13. Simulation results of the tail wing pitching moment M_{tail}

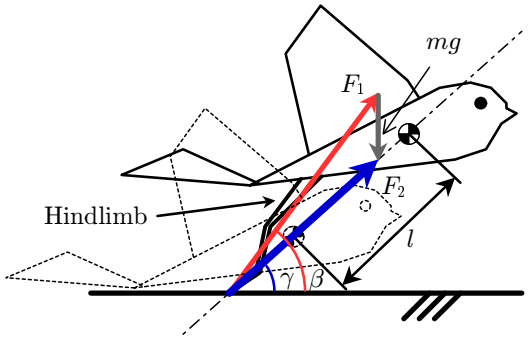

Fig. 14. Takeoff assisted by jumping with the hind limbs

flapping robot can be described by the forces F_x and F_z and the torque M_y about the y-axis of the robot measured with the force sensor as

$$M_{\mathrm{flg}} = \begin{bmatrix} -z_g & x_g & 1 \end{bmatrix} \begin{bmatrix} F_x \\ F_z \\ M_y \end{bmatrix}, \tag{5}$$

where x_g and z_g are the x- and z-coordinates, respectively, of the center of gravity in the force sensor coordinate system. Thus, the pitching moment $M_{\mathrm{flg}} = -59.0\,\mathrm{mNm}$ can be obtained from the above calculation. As a result, it is considered that the pitch angle decreased. When executing a flapping motion, moments are always generated to reciprocate a wing located some distance from the center of gravity. In the design of the DelFly, Olejnik et al. [7] implemented a method to control the moments using sweeping wings for stability. In contrast, general fixed-wing aircraft control the pitching moment via elevators in the tail wing. In the present experiment, the tail wing pitched upward at an angle of 25°. However, the pitching moment generated by the tail wing could not overcome the pitching moment generated by the flapping motion. Because the airspeed was low in the period immediately following takeoff, the tail wing did not generate a large pitching moment.

The pitching moment M_{tail} about the center of gravity generated by the tail wing is expressed as

$$M_{\mathrm{tail}} = \frac{1}{2}\rho S V^2 \left(C_M \bar{c} + C_L R\right), \tag{6}$$

where C_M is the pitching moment coefficient of the tail wing, C_L is its lift coefficient, $\bar{c}$ is its mean aerodynamic chord, and R is the distance from the aerodynamic center of the tail wing to the center of gravity of the robot. Fig. 13 shows the results of a simulation of the tail wing pitching moment, which indicate that the flapping robot must maintain a speed of 6.5 m/s to achieve horizontal flight. The pitching moment and lift coefficients of the triangular tail wing were $C_M = -0.15$ and $C_L = 0.75$ [7].

V. Discussion of the Actuated Hind Limbs

In the experiments discussed in the preceding chapter, takeoff was difficult in the proposed robot because the pitching moment generated by the flapping motion acts to decrease the pitch angle. The pitching moment produced by the tail wing was not enough to maintain a horizontal posture at low airspeeds during takeoff.

Most birds use their hind limbs to assist with takeoff. The hind limbs produce 80% to 90% of the takeoff speed when birds take off [5]. This indicates that the development of actuated hind limbs is necessary for the success of the developed flapping robot.

Zhang et al. [8] have proposed the method of jumping-aided takeoff. However, their estimation of the energy needed for jumping is not sufficient to consider the acceleration and final airspeed of the robot from the start of the jump. The energy was estimated herein with a focus on the final target airspeed.

In the design of the hind limbs, the following points should be considered. First, the final airspeed at the time of extension is approximately 90% of the airspeed. Additionally, the hind limbs should confer the ability to accelerate the flapping robot to the target airspeed, and their size and weight should be selected such that they are suitable for the body. The model of takeoff assist is shown in Fig. 14. It was assumed that the flapping robot has a constant mass m, final airspeed

V, expansion/contraction length l, kicking angle β, jumping angle γ, kicking force F_1 which is a reaction force generated by hind limbs kicking the ground, and jumping force F_2 which is a resultant force of kicking force F_1 and gravity force mg. The air resistance was ignored. The mechanical energy $F_2 l$ from the hind limbs and gravity can be expressed as follows:

$$F_2 l = \frac{1}{2} m V^2 + mgl \sin\gamma, \tag{7}$$

where the first and second terms on the right-hand side are the kinetic and potential energies, respectively, immediately after takeoff. The force F_1 and the duration of kicking t can be expressed as

$$F_1 = \sqrt{(F_2 \cos\gamma)^2 + (F_2 \sin\gamma + mg)^2}. \tag{8}$$

$$t = \frac{mV}{F_2} \tag{9}$$

The mechanical output P of the hind limbs can then be obtained as

$$P = (F_1 \cos(\beta - \gamma) l) / t \tag{10}$$

$$= \frac{l}{mV} F_1 F_2 \cos(\beta - \gamma) \tag{11}$$

It was assumed that the robot had a mass of $m = 0.1\,\mathrm{kg}$ because of the added mass of the hind limbs. The length of the hind limbs, $l = 0.19\,\mathrm{m}$, was estimated as half of the length of the body. The other parameters were set to $V = 4.95\,\mathrm{m/s}$ and $\gamma = 45°$. Based on these parameters, a simulation was performed, and a force of $F_1 = 7.8\,\mathrm{N}$ and a mechanical output of $P = 21.4\,\mathrm{W}$ were obtained. The parameters required for the development of the hind limbs were thus obtained. The inclusion of hind limbs in this manner could be possible, because the weight of the present reducer including 36 W BLDC motor is enough lightweight of 14 g.

VI. Conclusion

The aim of this study was to develop a flapping robot capable of self-takeoff without running. An experiment on the static thrust of the robot revealed that it was able to generate a thrust exceeding its own weight. The drag coefficient was obtained from the rate of descent during gliding, and the airspeed achieved by the thrust generated from flapping was simulated. The results confirmed that the robot is capable of reaching the target airspeed during takeoff. The results of the takeoff experiment also revealed the actual airspeed of the developed robot. Thus, it was determined that the developed flapping robot has the basic ability for self-takeoff without running.

Experiments were conducted with the flapping robot taking off with various initial pitch angles. The results demonstrated that takeoff was possible if the initial pitch angle was high. However, the pitch angle decreased immediately after takeoff. From the force sensor data, it was found that the pitching moment that caused this decrease in the pitch angle was generated by the flapping motion. The pitching moment about the center of gravity generated by the tail wing was estimated and found to be less than the pitching moment generated by the flapping motion. The pitching moment generated by the tail wing was not sufficient to maintain a horizontal posture at low airspeeds during takeoff.

It was concluded that the robot must include a control mechanism for the pitching moment generated by the flapping motion and/or an accelerator without flapping applied during takeoff, such as hind limbs. Therefore, the parameters required for the design of actuated hind limbs were estimated.

References

[1] M. F. Bin Abas, A. S. Bin Mohd Rafie, H. Bin Yusoff, and K. A. Bin Ahmad, "Flapping wing micro-aerial-vehicle: Kinematics, membranes, and flapping mechanisms of ornithopter and insect flight," *Chinese Journal of Aeronautics*, vol. 29, no. 5, pp. 1159–1177, 2016.

[2] M. Keennon, K. Klingebiel, and H. Won, "Development of the nano hummingbird: A tailless flapping wing micro air vehicle," in *50th AIAA Aerospace Sciences Meeting Including the New Horizons Forum and Aerospace Exposition*, Jan 2012.

[3] C. De Wagter, S. Tijmons, B. D. W. Remes, and G. C. H. E. de Croon, "Autonomous flight of a 20-gram flapping wing mav with a 4-gram onboard stereo vision system," in *IEEE ICRA2014*, May 2014, pp. 4982–4987.

[4] G. Ise *et al.*, "Controlling the aerial posture of a flapping-wing micro air vehicle by shifting its centre of gravity," in *10th International Micro Air Vehicle Competition and Conference*, Melbourne, Australia, Nov 2018, pp. 211–215.

[5] K. D. Earls, "Kinematics and mechanics of ground take-off in the starling Sturnis vulgaris and the quail Coturnix coturnix," *Journal of Experimental Biology*, vol. 203, no. 4, pp. 725–739, 2000.

[6] H. Tennekes, *The Simple Science of Flight: From Insects to Jumbo Jets*. MIT Press, 2009.

[7] M. Okamoto and Y. Jinba, "Experimental study on aerodynamic characteristics of wing planforms at low reynolds number," *Research reports of Akita National College of Technology(in Japanese)*, no. 44, pp. 42–50, Feb 2009.

[8] J. Zhang, C. Dong, and A. Song, "Jumping Aided Takeoff : Conceptual Design of A Bio-Inspired Jumping-Flapping Multi-Modal Locomotion Robot," in *Proc. IEEE ROBIO2017*, 2017, pp. 32–37.